NIH Public Access
Author Manuscript
Neurobiol Aging. Author manuscript; available in PMC 2013 August 01.

Published in final edited form as:
Neurobiol Aging. 2012 August ; 33(8): 1507–1521. doi:10.1016/j.neurobiolaging.2011.03.001.

Ovarian hormone loss induces bioenergetic deficits and mitochondrial β-amyloid

Jia Yao[a], **Ronald Irwin**[a], **Shuhua Chen**[a], **Ryan Hamilton**[a], **Enrique Cadenas**[a], and **Roberta Diaz Brinton**[a,b]

[a]Department of Pharmacology and Pharmaceutical Sciences, School of Pharmacy, University of Southern California, Los Angeles, California 90033

[a]Department of Neurology, Keck School of Medicine, University of Southern California, Los Angeles, California 90033

Abstract

Previously, we demonstrated that reproductive senescence was associated with mitochondrial deficits comparable to those of female triple-transgenic Alzheimer's mice (3xTgAD). Herein, we investigated the impact of chronic ovarian hormone deprivation and 17β-estradiol (E2) replacement on mitochondrial function in non-transgenic (nonTg) and 3xTgAD female mouse brain. Depletion of ovarian hormones by ovariectomy (OVX) in nonTg mice significantly decreased brain bioenergetics, and induced mitochondrial dysfunction and oxidative stress. In 3xTgAD mice, OVX significantly exacerbated mitochondrial dysfunction and induced mitochondrial β-amyloid and Aβ−binding-alcohol-dehydrogenase (ABAD) expression. Treatment with E2 at OVX, prevented OVX-induced mitochondrial deficits, sustained mitochondrial bioenergetic function, decreased oxidative stress, and prevented mitochondrial β-amyloid and ABAD accumulation. *In vitro*, E2 increased maximal mitochondrial respiration in neurons and basal and maximal respiration in glia. Collectively, these data demonstrate that ovarian hormone loss induced a mitochondrial phenotype comparable to a transgenic female model of AD, which was prevented by E2. These findings provide a plausible mechanism for increased risk of AD in premenopausally oophorectomized women while also suggesting a therapeutic strategy for prevention.

Keywords

mitochondria; bioenergetics; estrogen; Alzheimer's; ovariectomy; oxidative stress

1. Introduction

The essential role of mitochondria in cellular bioenergetics and survival has been well established (Brinton, 2008, Magistretti, 2006, Wallace, 2005). Further, mitochondrial

© 2011 Elsevier Inc. All rights reserved.

Corresponding Author: Roberta Diaz Brinton, Department of Pharmacology and Pharmaceutical Sciences, University of Southern California, School of Pharmacy, Los Angeles, CA 90033. rbrinton@usc.edu, Tel: 323-442-1436, Fax: 323-442-1470.

Publisher's Disclaimer: This is a PDF file of an unedited manuscript that has been accepted for publication. As a service to our customers we are providing this early version of the manuscript. The manuscript will undergo copyediting, typesetting, and review of the resulting proof before it is published in its final citable form. Please note that during the production process errors may be discovered which could affect the content, and all legal disclaimers that apply to the journal pertain.

Disclosure statement
No conflicts of interest for all authors

NIH-PA Author Manuscript
NIH-PA Author Manuscript
NIH-PA Author Manuscript

NIH-PA Author Manuscript

NIH-PA Author Manuscript

NIH-PA Author Manuscript

dysfunction has been suggested to play a pivotal role in neurodegenerative disorders, including Alzheimer's disease (AD) (Brinton, 2008, Moreira, et al., 2010, Mosconi, et al., 2009, Swerdlow and Khan, 2009). Recently we demonstrated that mitochondrial bioenergetic deficits precede Alzheimer's pathology in the female triple transgenic mouse model of Alzheimer's disease (3xTgAD), suggesting a causal role of mitochondrial bioenergetic deficiency in AD pathogenesis (Yao, et al., 2009). In the female 3xTgAD mouse brain mitochondrial dysfunction was evidenced by decreased mitochondrial respiration, decreased metabolic enzyme expression and activity, increased oxidative stress, and increased mitochondrial Aβ load and Aβ−binding-alcohol-dehydrogenase (ABAD) expression. Further, we demonstrated that mitochondrial dysfunction was evident following natural reproductive senescence in normal aging mice and was exacerbated in 3xTgAD mice (Yao, et al., 2010, Yao, et al., 2009). Findings from these pre-clinical animal studies are consistent with the clinical observation that menopause is associated with a decline in brain metabolism in women whereas women who received hormone therapy did not show a decline in brain metabolism (Maki and Resnick, 2001, Rasgon, et al., 2005).

Basic science analyses have suggested that many of the neuroprotective mechanisms of ovarian hormones converge upon mitochondria (Brinton, 2008, Simpkins and Dykens, 2008). Estrogen promotes mitochondrial bioenergetics, protects against free radical damage, and decreases Aβ while upregulating Aβ degrading enzymes (Brinton, 2009, Carroll, et al., 2007, Nilsen, et al., 2007, Petanceska, et al., 2000, Simpkins, et al., 2009, Zhao, et al., 2010). Further, estrogen increases expression and activity of proteins involved in oxidative phosphorylation, including pyruvate dehydrogenase, aconitase, and ATP synthase (Nilsen, et al., 2007). Epidemiological analyses indicate that hormone therapy at the menopause transition can reduce the risk of Alzheimer's disease in postmenopausal women (Henderson, 2010) whereas women not receiving hormone therapy following surgically-induced menopause are at increased risk for Alzheimer's disease (Rocca, et al., 2007, Rocca, et al., 2010).

In the current study, we sought to determine the relationship between impact of long-term chronic deprivation of ovarian hormones on mitochondrial function in both normal and 3xTgAD female mouse brains. We also investigated the efficacy of 17β-estradiol (E2) to prevent ovariectomy (OVX) induced deficits in mitochondrial function. We further differentiated the neuronal versus glial contribution to E2 regulation of brain metabolism. Results of these analyzes demonstrate that loss of ovarian hormones induced a significant decline in mitochondrial bioenergetics paralleled by a significant increase in oxidative stress, mitochondrial fission and mitochondrial localization of Aβ which were all prevented by E2 treatment at time of OVX. Because hypometabolism in brain is an early indicator of increased risk for AD (Mosconi, et al., 2006, Reiman, et al., 2005), findings from this study provide potential mechanisms for the higher life-time risk for AD in postmenopausal women (Alzheimer's Association, 2010). These data indicate a therapeutic strategy that targets mitochondria to prevent or delay menopause-associated mitochondrial deficits associated with increased risk of AD in premenopausally oophorectomized women (Rocca, et al., 2010).

2. Materials and Methods

2.1 Transgenic Mice

Colonies of 3xTgAD and nonTg mouse strain (C57BL6/129S; Gift from Dr. Frank Laferla, University of California, Irvine) (Oddo, et al., 2003) were bred and maintained at the University of Southern California (Los Angeles, CA) following National Institutes of Health guidelines on use of laboratory animals and an approved protocol by the University of Southern California Institutional Animal Care and Use Committee. Mice were housed on 12

NIH-PA Author Manuscript

NIH-PA Author Manuscript

NIH-PA Author Manuscript

h light/dark cycles and provided *ad libitum* access to food and water. The characterization of amyloid and tau pathologies, as well as synaptic dysfunction in this line of mice has been described previously (Oddo, et al., 2003) and confirmed in our laboratory. Mice were genotyped routinely to confirm the purity of the colony. To ensure the stability of AD-like phenotype in the 3xTgAD mouse colony, we performed routine immunohistochemical assays every three to four generations. Only offspring from breeders that exhibit stable AD pathology were randomized into the study.

2.2 Experimental Design

To investigate the change in mitochondrial function following removal of ovaries and treatment with 17β-estradiol (E2), 3 month old female 3xTgAD and nonTg mice were randomly assigned to one of the following three treatment groups (n=10 per group): sham ovariectomized (Sham-OVX), ovariectomized (OVX), and OVX plus 17β-estradiol (OVX +E2). Mice were bilaterally OVX and immediately implanted with a continuous 90 day release pellet (Innovative Research of America, Sarasota FL) containing either 0.25 mg of E2 (OVX+E2 group) or steroid free control pellets (Sham-OVX and OVX groups). All the mice were sacrificed at 6 month, 90 days after the initiation of experimental interventions.

2.3 Brain Tissue Preparation and Mitochondrial Isolation

Upon completion of E2 treatment, both 3xTgAD and nonTg groups (n=7 per group) were sacrificed and the brains rapidly dissected on ice. Cerebellum and brain stem was removed from each brain and the hippocampus within the left hemisphere was harvested for future analysis. Brain mitochondria were isolated from the remainder (whole brain minus cerebellum and brain stem) following our previously established protocol (Irwin, et al., 2008). The brain was rapidly minced and homogenized at 4°C in mitochondrial isolation buffer (MIB) (PH 7.4), containing sucrose (320 mM), EDTA (1 mM), Tris-HCl (10mM), and Calbiochem's Protease Inhibitor Cocktail Set I (AEBSF-HCl 500μM, aprotonin 150 nM, E-64 1 μM, EDTA disodium 500 μM, leupeptin hemisulfate 1 μM). Single-brain homogenates were then centrifuged at 1500 X g for 5 min. The pellet was resuspended in MIB, rehomogenized, and centrifuged again at 1500 X g for 5 min. The postnuclear supernatants from both centrifugations were combined, and crude mitochondria were pelleted by centrifugation at 21,000 X g for 10 min. The resulting mitochondrial pellet was resuspended in 15% Percoll made in MIB, layered over a preformed 23%/40% Percoll discontinuous gradient, and centrifuged at 31,000 X g for 10 min. The purified mitochondria were collected at the 23%/40% interface and washed with 10 ml MIB by centrifugation at 16,700 X g for 13 min. The loose pellet was collected and transferred to a microcentrifuge tube and washed in MIB by centrifugation at 9000 X g for 8 min. The resulting mitochondrial pellet was resuspended in MIB to an approximate concentration of 1mg/ml. The resulting mitochondrial samples were used immediately for respiratory measurements and hydrogen peroxide production or stored at −80°C for later protein and enzymatic assays. During mitochondrial purification, aliquots were collected for confirmation of mitochondrial purity and integrity following previously established protocols (Irwin, et al., 2008, Nilsen, et al., 2007). Briefly, Western blot analysis was performed for mitochondrial anti-VDAC (1:500; Mitosciences, Eugene, OR), nuclear anti-histone H1 (1:250; Santa Cruz Biotechnology, Santa Cruz, CA), endoplasmic reticulum anti-calnexin (1:2000, SPA 865; Stressgen, now a subsidiary of Assay Designs, Ann Arbor, MI), and cytoplasmic anti-myelin basic protein (1:500, clone 2; RDI, Concord, MA) (data not shown).

2.4 Immunohistochemistry

For immunohistochemistry studies, animals (n=3 per group) were sacrificed, brains were perfused with pre-chilled PBS buffer (pH 7.2) and immersion fixed in 4% paraformaldehyde for 48 h and then stored in 4°C in PBS/1% sodium azide until use. Fixed brains were sent to

NIH-PA Author Manuscript

NIH-PA Author Manuscript

NIH-PA Author Manuscript

Neuroscience Associates (NSA, Knoxville, TN) for coronal sectioning at 35μm, and then processed for immunohistochemistry using a standard protocol. Briefly, every 12th section was blocked (1h at RT, PBS with 5% goat serum and 0.3 % trinton x-100), immunostained using antibody directed against Aβ (6E10, Signet 1:1000 dilution 4°C overnight) followed by washing and secondary antibody Fluorescein goat anti-mouse (1:500, Chemicon, Ramona, CA, 1h at RT). Sections were mounted with anti-fade mounting medium with DAPI (Vector Laboratories, Burlingame, CA). Antigen unmasking treatment, consisting of 5 min rinse in 99% formic acid was performed to enhance Aβ immunoreactivity (IR). Fluorescent images were taken using a fluorescent microscope, normalized and analyzed with the slide book software (Intelligent Imaging Innovations Inc, Santa Monica, CA).

2.5 Western Blot Analysis

Protein concentrations were determined by using the BCA protein assay kit (Pierce, Rockford, IL). Equal amounts of proteins (20 μg/well) were loaded in each well of a 12% SDS-PAGE gel, electrophoresed with a Tris/glycine running buffer, and transferred to a 0.45μm pore size polyvinylidene difluoride (PVDF) membrane and immunobloted with PDH E1 alpha antibody (1:1000, Mitosciences, Eugene, OR), COX IV antibody (1:2000, Mitosciences, Eugene, OR), ABAD antibody (1:1000, Abcam, Cambridge, MA), β-actin antibody (1:4000, Chemicon, Ramona, CA), OPA1 antibody (1:1000, BD Biosciences, San Jose, CA), Drp1/Dlp1 antibody (1:1000, BD Biosciences, San Jose, CA) and porin/VDAC antibody (1:500, Cell Signaling, Danvers, MA). Mitochondrial Aβ oligomer (16KD) level was determined in isolated mitochondrial samples (20μg/well) and blotted by specific anti-Aβ monoclonal antibody (6E10, Signet). HRP-conjugated anti-rabbit antibody and HRP-anti-mouse antibody (Vector Laboratories, Burlingame, CA) were used as secondary antibodies. Immunoreactive bands were visualized by Pierce SuperSignal Chemiluminescent Substrates (Thermo Scientific) and captured by Molecular Imager ChemiDoc XRS System (Bio-Rad, Hercules, CA). All band intensities were quantified using Un-Scan-it software (Silk Scientific, Orem, UT).

2.6 Enzyme Activity Assay

PDH activity was measured by monitoring the conversion of NAD+ to NADH by following the change in absorption at 340 nm as previously described (Yao, et al., 2009). Isolated brain mitochondria were dissolved in 2% CHAPS buffer to yield a final concentration of 15 μg/μl and incubated at 37°C in PDH Assay Buffer (35 mM KH_2PO_4, 2 mM KCN, 0.5 mM EDTA, 5 mM $MgCl_2$, (pH 7.25 with KOH), 200 mM sodium pyruvate, 2.5 mM rotenone, 4 mM sodium CoA, 40 mM TPP). The reaction was initiated by the addition of 15 mM NAD^+. COX activity was assessed in isolated mitochondria (20 μg) using Rapid Microplate Assay kit for Mouse Complex IV Activity (Mitosciences, Eugene, OR) following the manufacturer's instructions. Complex I Activity assessed in isolated mitochondrial samples (5 ug) using Complex I Enzyme Activity Dipstick Assay Kit (Mitosciences, MS130-60, Eugene, OR), band density was captured and analyzed by the matching Mitosciences Dipstick reader (Mitosciences, MS1000, Eugene, OR).

2.7 Lipid Peroxidation

Lipid peroxides in brain mitochondria and hippocampal lysates were assessed using the leucomethylene blue assay, using *tert*-butyl hydroperoxide as a standard, by monitoring the 650 nm absorbance after 1 h incubation at RT. The aldehyde product or termination production of lipid peroxidation in brain mitochondria was determined by measuring thiobarbituric acid reactive substances (TBARS). Samples were mixed with 0.15 M phosphoric acid. After the addition of thiobarbituric acid, the reaction mixture was heated to 100°C for 1 h. After cooling and centrifugation, the formation of TBARS was determined by

NIH-PA Author Manuscript

NIH-PA Author Manuscript

NIH-PA Author Manuscript

the absorbance of the chromophore (pink dye) at 531 nm using 600 nm as the reference wavelength.

2.8 8-oxoGuannine Quanitification

Serum samples were collected from the animals upon completion of the study. Briefly, 0.5 ml of blood was collected from each animal. Blood samples were allowed to clot at RT for 30 min and then centrifuged at 2200 × g for 10 min. Serum samples were collected from the supernatant and stored at −80°C. Serum 8-oxoGuanine level was determined using the OxiSelect™ oxidative RNA Damage ELISA (8-oxoGuanine Quantitation) assay kit (Cellbiolabs, San Diego, CA) following the product manual.

2.9 Respiratory Measurement

Mitochondrial respiration was measured using MitoXpress™ fluorescent dye from isolated mitochondria following a previously established protocol (Will, et al., 2006). Briefly, 50 μg of isolated mitochondria were diluted to 1 μg/μl with respiratory buffer (250 mM sucrose, 15 mM KCl, 1 mM EGTA, 5 mM $MgCl_2$, 30 mM KH_2PO_4, pH 7.4) and added to test well. MitoXpress™ probe was reconstituted into 1μM stock solution and further diluted 1:10 in respiration buffer. State 4 respiration was stimulated with the addition of glutamate (5 mM) and malate (5 mM) as substrates. State 3 respiration was stimulated by the addition of glutamate (5 mM) and malate (5 mM) plus ADP (410 μM). The rate of oxygen consumption was calculated based on the slope of the response of isolated mitochondria to the successive administration of substrates. 100 μl mineral oil was added to each well promptly after the addition of MitoXpress working solution into the well. MitoXpress signal was measured at 1min intervals for 60 min using excitation and emission wavelength of 380 nm and 650 nm respectively. To determine the rate of respiration, fluorescence-time profiles were linearized using the following coordinate scale: Abscissa, Y: $I(t_0)/(I(t)-I(t_0))$, where $I(t_0)$ and I(t) represent fluorescence intensity signals at the start and at time (t) of monitoring, respectively; Ordinate, X: 1/t, min^{-1}; exclude zero time points and regions of signal saturation, i.e., long monitoring times. Linear regression analysis was applied to the transformed profiles to determine the slope and correlation coefficient for each of the transformed profiles. State 4 and State 3 respiration rate were calculated as the reciprocal ratio of the above two calculated slopes, respectively. The respiratory control ratio (RCR) was defined by dividing the rate of oxygen consumption/min for State 3 (presence of ADP) by the rate of oxygen consumption/min for State 4 respiration.

2.10 Mitochondrial Biogenesis

Total DNA was isolated with Wizard Genomic DNA Purification Kit (Promega, Madison, WI) and analyzed by real-time PCR. Mitochondrial biogenesis was estimated as the relative levels of COXII DNA to β-actin.

2.11 Metabolic Flux Analysis

Primary hippocampal neurons from day 18 (E18) embryos of female Sprague-Dawley rats were cultured on Seahorse XF-24 plates at a density of 50,000 cells/well. Neurons were grown in Neurobasal Medium +B27 supplement for 10 days prior to experiment. Mixed glia from day 18 (E18) embryos of female Sprague-Dawley rats were cultured in T75 flasks and grown in growth media (DMEM:F12 (1:1), phenol red free +10% FBS). 24 hour prior to the experiment, mixed glia were trypsinized and seeded onto Seahorse XF-24 plates at a density of 50,000 cells/well in growth media. For basal respiration comparison between neurons and mixed glia, cells were proceeded to assays directly. To investigate the impact of E2 treatment on mitochondrial respiration in cell cultures, cells were treated with control vehicle or E2 and the assays were conducted 24 h post-treatment. Neurons were treated with

NIH-PA Author Manuscript

NIH-PA Author Manuscript

NIH-PA Author Manuscript

control vehicle or E2 in Neurobasal Medium. For E2 treatment in mixed glial cells, full growth media were replaced with DMEM: F12 (1:1) without FBS to eliminate the interference from serum. On the day of metabolic flux analysis, media was changed to unbuffered DMEM (DMEM Base medium supplemented with 25 mM glucose, 1 mM sodium pyruvate, 31 mM NaCl, 2 mM GlutaMax; pH 7.4) and incubated at 37°C in a non-CO_2 incubator for 1 h. All medium and injection reagents were adjusted to pH 7.4 on the day of assay. Using the Seahorse XF-24 metabolic analyzer, four baseline measurements of OCR (oxygen consumption rate) and ECAR (extracellular acidification rate) were sampled prior to sequential injection of mitochondrial inhibitors. Three metabolic determinations were sampled following addition of each mitochondrial inhibitor prior to injection of the subsequent inhibitors. The mitochondrial inhibitors used were oligomycin (1 μM), FCCP (1 μM), and rotenone (1 μM). OCR and ECAR were automatically calculated and recorded by the Seahorse XF-24 software. After the assays, protein level was determined for each well to confirm equal cell density per well. The percentage of change relative to the basal rate was calculated as the value of change divided by the average value of baseline.

2.12 Statistics

Statistically significant differences between groups were determined by student t-test (for Seahorse metabolic flux assays) or one way ANOVA followed by a Newman-Keuls posthoc analysis (for other analyses).

3. Results

3.1 Brain-independent confirmation of ovarian hormone status

The same experiment model has been previously demonstrated to successfully deliver physiological E2 levels by directly measuring serum E2 levels (Carroll, et al., 2007). In the current study, uterine weight was used as a bioassay to confirm depletion of ovarian hormones and 17β-estradiol (E2) treatment in female nonTg and 3xTgAD mice. In both nonTg and 3xTgAD mice, OVX-induced hormone depletion resulted in a significant decrease in uterine weight relative to the Sham-OVX group whereas E2 treatment induced a significant increase compared to the OVX group (Table 1, $P<0.05$). Changes in uterine weight were independent indicators for the efficacy of experimental OVX and E2 treatments in both nonTg and 3xTgAD mice.

3.2 Ovariectomy-induced decrease in mitochondrial respiration and prevention by 17β-estradiol (E2)

Mitochondrial respiration is a direct indicator of overall metabolic activity. To investigate the impact of chronic ovarian hormone loss and E2 (0.25mg/90 days pellet) exposure on mitochondrial respiration, whole forebrain (whole brain minus cerebellum and brain stem) mitochondria were isolated from both nonTg and 3xTgAD female mice following 3 months of Sham-OVX, OVX or OVX+E2 exposure and measured for mitochondrial respiration. Consistent with our previous findings, in the Sham-OVX groups, 3xTgAD mice exhibited lower respiratory control ratio (RCR) relative to nonTg mice (Fig. 1B and 1D) (Yao, et al., 2009). More importantly, relative to ovary-intact mice (Sham-OVX), RCR was significantly decreased by OVX in both nonTg (~30%) and 3xTgAD (~40%) group (Fig.1, $P<0.05$, compared to Sham-OVX group, n=7). The changes in RCR were due to a deficit in State 3 respiration in both nonTg and 3xTgAD mice as OVX significantly decreased the rate of State 3 respiration whereas there was no significant difference in the rate of State 4 respiration in either group (Fig. 1A and 1C). Treatment with E2 initiated immediately at time of OVX prevented the OVX-induced decline in State 3 mitochondrial respiration in both the nonTg and 3xTgAD groups (Fig. 1A and 1C; $P<0.05$, compared to OVX, n=7) and maintained mitochondrial respiration at a level comparable to Sham-OVX. Further, OVX

NIH-PA Author Manuscript

NIH-PA Author Manuscript

NIH-PA Author Manuscript

specifically decreased ADP dependent State 3 respiration which was prevented by E2 treatment. This finding indicates that E2 functions to promote efficiency of mitochondrial respiration rather than regulating mitochondrial proton flux as no significant change in State 4 respiration was observed.

3.3 Ovariectomy-induced decrease in mitochondrial metabolic enzyme activity and prevention by 17β-estradiol

To investigate the impact of ovariectomy and E2 on mitochondrial enzymes involved in metabolism and respiration, we assessed activities of PDH, complex I (NADH dehydrogenase), and complex IV (cytochrome c oxidase). PDH is the key enzyme linking glycolysis to oxidative phosphorylation (OXPHOS); Complex I controls the entry of electron flow to the mitochondrial electron transport chain (mETC), hence controlling the entry point of OXPHOS in brain; Complex IV is the terminal enzyme of electron flow and reduces O_2 to H_2O. Activity of PDH and COX is significantly decreased in postmortem Alzheimer's brain tissue (Blass, et al., 2000, Martins and Hallmayer, 2004) whereas Complex I activity is compromised in Parkinson's disease (Beal, 2005). In nonTg female mice, OVX induced a significant decline in PDH activity, while E2 treatment prevented the OVX-induced decline and sustained PDH activity to a level comparable to the Sham-OVX group (Fig. 2A). Similarly, in 3xTgAD female mice, OVX also induced a significant decline in PDH activity while E2 treatment induced a partial but not statistically significant prevention against the OVX-induced decline in PDH activity (Fig. 2A). OVX induced significant decrease in COX activity in 3xTgAD mice and a similar but not significant trend of decline in nonTg mice, while E2 treatment induced a significant increase in COX activity in nonTg mice and a similar but not significant trend of increase in 3xTgD mice (Fig. 2D). In both nonTg and 3xTgAD mice, E2 prevented the OVX-induced decline in mitochondrial function to the extent that there was no statistical significance between the OVX+E2 group and the ovary-intact animals (Sham-OVX) (Fig. 2A & 2D). Unlike PDH and COX, Complex I activity was not significantly affected although it followed the same trend as PDH and COX with OVX inducing a decline which was prevented by E2 in both nonTg and 3xTgAD mice (Fig. 2B). The OVX-induced decrease in PDH activity would predict decreased generation of acetyl-CoA, which would, in turn, predict a decline in citric acid cycle generated NADH required for oxidative phosphorylation. A decline in NADH generated proton gradient would be reflected by a decline in ATP generation which would be further exacerbated by a decline in COX activity.

3.4 Ovariectomy-induced increase in oxidative stress in brain and prevention by 17β-estradiol

Efficiency of coupled electron transport is directly related to generation of oxidative damage in mitochondria. To determine the impact of loss of ovarian hormones and E2 treatment on oxidative stress, we assessed the magnitude of lipid peroxidation of isolated brain mitochondria and hippocampal lysates as an indicator of oxidative damage to cellular components. In addition, we assessed the serum level of oxidized RNA as indicated by 8-oxoGuanine (8-OHG). Loss of ovarian hormones induced a significant rise in mitochondrial lipid peroxidation in both nonTg and 3xTgAD female mice relative to corresponding Sham-OVX groups (Fig. 3A). E2 treatment prevented OVX-induced lipid peroxidation in both nonTg and 3xTgAD mice (Fig.3A). Lipid peroxidation within hippocampal lysates yielded comparable results (Fig. 3B). Likewise, OVX induced a significant increase in serum 8-OHG level in both nonTg and 3xTgAD mice, which was also prevented by E2 treatment (Fig. 3C, $P<0.05$, $n=10$). This finding indicates that the rise in oxidative stress induced by loss of ovarian hormones is not limited to brain or to lipid membranes but can include oxidation of RNA. Likewise, the antioxidant effect of E2 was evident in both brain and plasma.

NIH-PA Author Manuscript

NIH-PA Author Manuscript

NIH-PA Author Manuscript

3.5 Ovariectomy-induced rise in brain and mitochondrial amyloid load and prevention by 17β-estradiol

Previous studies indicated that amyloid beta (Aβ) interacts with a mitochondrial protein, amyloid beta binding alcohol dehydrogenase (ABAD), and that binding of Aβ with ABAD contributes to mitochondrial dysfunction (Lustbader, et al., 2004, Takuma, et al., 2005). In the 3xTgAD mouse model, we previously demonstrated that Aβ was present in brain mitochondria derived from ovary-intact 9-month old female 3xTgAD mice and was associated with increased ABAD expression (Yao, et al., 2009). To investigate whether loss of ovarian hormones leads to mitochondrial Aβ accumulation and ABAD over-expression, mitochondrial samples from Sham-OVX, OVX, and OVX+E2 groups of 3xTgAD mice were analyzed by western blot for mitochondrial Aβ and ABAD expression. Ovariectomy of 3xTgAD mice induced a significant increase in mitochondrially localized Aβ and ABAD expression (Fig. 4A and 4B, $P<0.05$, n=7). Treatment with E2 prevented the OVX-induced increase in mitochondrial Aβ and ABAD load (Fig. 4A and 4B, $P<0.05$, n=7), although mitochondrial Aβ level in the OVX+E2 group was still higher than the Sham-OVX group. As loss of ovarian hormones is known to increase Aβ load in brain (Carroll, et al., 2007, Petanceska, et al., 2000), we sought to determine whether mitochondrial Aβ correlated with overall Aβ load in hippocampus. Immunocytochemical labeling of Aβ was conducted in hippocampal brain sections derived from Sham-OVX, OVX and OVX+E2 treated 3xTgAD mice. Similar to findings of mitochondrial Aβ load, immunofluorescent labeling revealed a qualitative increase in 6E10 labeling of Aβ in the hippocampal CA1 region of the OVX group relative to the Sham-OVX group, whereas OVX+E2 group exhibited lower 6E10 immunoreactivity that was comparable to Sham-OVX (Fig. 4C).

3.6 Altered mitochondrial dynamics with ovariectomy and E2 treatment with no impact on mitochondrial content

Mitochondrial dynamics of fission, fusion and biogenesis, are associated with mitochondrial respiratory efficiency, enzyme expression and activity and have been proposed as contributing to the bioenergetic phenotype of Alzheimer's and Parkinson's disease (Chan, 2006, Wang, et al., 2009). To investigate the impact of long-term ovarian hormone deprivation and E2 treatment on mitochondrial dynamics, we first assessed expression of markers of mitochondrial fission and fusion. As an indicator of mitochondrial fission, the cytoplasmic mitochondrial tubule localized protein dynamin-related protein 1 (Drp1) was assessed. To assess mitochondrial fusion, optic atrophy 1 (OPA1) which is involved in the fusion of inner mitochondrial membranes was assessed (Mattson et al., 2008). Ovariectomy induced a significant increase in expression of the fission protein, Drp1 (Fig. 5A, $P<0.05$) and a significant decrease in expression of the fusion protein, OPA1, (Fig. 5B, $P<0.05$) in isolated mitochondrial samples from both nonTg and 3xTgAD mice. E2 treatment at time of OVX prevented OVX-induced increase in Drp1 and decrease in OPA1 expression (Fig. 5A & 5B, $P<0.05$) to a level comparable to the respective Sham-OVX group. Because altered mitochondrial dynamics can be a prelude to changes in mitochondrial biogenesis (Mattson et al., 2008), we investigated the impact of long-term ovarian hormone depletion on mitochondrial biogenesis. We assessed the ratio of mitochondrial DNA (mtDNA) to nuclear DNA as a marker of mitochondrial biogenesis. Real-time PCR for COXII (mitochondrial DNA encoded) and β-actin (nuclear DNA encoded) was performed on total genomic DNA isolated from cerebral cortex. Results of these analyses demonstrated no significant difference in the ratio of COXII to β-actin between Sham-OVX, OVX or OVX+E2 group in both nonTg and 3xTgAD mice (Fig. 5C), indicating that neither ovariectomy nor E2 altered the rate of mitochondrial biogenesis. Collectively these data indicate that loss of ovarian hormones shifts mitochondrial dynamics towards fission and away from fusion with no significant impact on mitochondrial biogenesis, whereas E2 treatment prevented the OVX-induced shift towards fission in mitochondrial dynamics.

NIH-PA Author Manuscript

NIH-PA Author Manuscript

NIH-PA Author Manuscript

3.7 17β-Estradiol differentially regulates mitochondrial bioenergetics in neurons and glia

To determine the cellular contribution to estrogen-inducible mitochondrial bioenergetics, we investigated E2 regulation of mitochondrial respiration in primary neuronal and glial cultures. In both primary neurons and mixed glia >80% of OCR measured was due to oxidative phosphorylation as indicated by the decrease (>80% decrease relative to basal level) in OCR with the addition of the Complex I inhibitor rotenone. The addition of the ATP synthase inhibitor oligomycin (1 μM) resulted in ~70% decrease in OCR in neurons and ~60% decrease in OCR in mixed glia (Fig. 6A), indicating that oxygen consumption was largely driven by oxidative phosphorylation-coupled ATP generation. Direct comparison of primary neurons and mixed glia revealed a 1.6 fold higher basal OCR in neurons compared to mixed glia indicating that neurons are highly oxidative whereas glial cells exhibit a less-oxidative phenotype. This observation is consistent with the difference in function between neurons and glia. Neurons have a greater bioenergetic demand based on the requirement to rapidly transport ions against their concentration gradient to re-establish membrane potential whereas astrocytes perform glycolysis and provide substrates for neurons (Belanger and Magistretti, 2009, Magistretti, 2006). Consistent with the bioenergetic demand, neurons exhibited significantly higher maximal mitochondrial respiratory capacity relative to mixed glia (Fig. 6A, $P<0.05$) as evidenced by the increase in OCR with the addition of a mitochondrial uncoupler (FCCP, 1μM) which reflects the maximal reserved respiratory capacity of mitochondria. To investigate E2 regulation of mitochondrial bioenergetics, both neurons and mixed glia were treated with E2 (10ng/ml) for 24 hours. Comparison of mitochondrial respiration between E2 treated neurons and mixed glia demonstrated differential regulation by E2. In neurons, E2 significantly increased the maximal reserved respiratory capacity without affecting basal respiration (Fig. 6B, $P<0.05$) whereas in mixed glia, E2 significantly increased both the maximal reserved respiratory capacity and basal respiration (Fig. 6C, $P<0.05$). In neurons, E2 treatment did not significantly increase ECAR (Fig. 6B). In contrast, E2 treatment significantly increased glycolysis in mixed glia as ECAR was significantly increased (Fig. 6C, $P<0.05$)

4. Discussion

In this study, we investigated the impact of long-term ovarian hormone deficiency on brain mitochondrial function and bioenergetics in both normal nonTg and 3xTgAD female mice. Results of these analyses indicated that long-term ovarian hormone deficiency induced by OVX prior to reproductive senescence resulted in a significant decrease in mitochondrial function in both nonTg and 3xTgAD brains. Specifically, OVX decreased brain mitochondrial respiration, increased oxidative stress and decreased expression and activity of mitochondrial metabolic enzymes. Further, OVX induced an increase in mitochondrial fission and a decline in mitochondrial fusion in both nonTg and 3xTgAD brains. In 3xTgAD mice, OVX induced an increase in mitochondrial Aβ load and a significant induction of ABAD protein expression. These data indicate that the decline in mitochondrial function associated with reproductive senescence (Yao, et al., 2009) is due to loss of ovarian hormones. Further, the current findings provide a plausible mechanism underlying the clinical observation of increased risk of Alzheimer's in women who have undergone oophorectomy prior to menopause (Rocca, et al., 2010).

Mitochondrial oxidative phosphorylation is the major generator of cellular ATP in brain (Reddy and Beal, 2008) and perturbations of brain mitochondrial bioenergetics will inevitably compromise brain metabolism (Swerdlow and Khan, 2009). Previous studies have shown that compared to nonTg mice, 3xTgAD mice exhibit decreased mitochondrial bioenergetics and brain glucose metabolism (Nicholson, et al., 2010, Yao, et al., 2009). Further, OVX can induce a decrease in brain glucose consumption in a rodent model (Lopez-Grueso, et al., 2010). Clinical positron emission topography (PET) analyses indicate

NIH-PA Author Manuscript

NIH-PA Author Manuscript

NIH-PA Author Manuscript

that menopausal women who did not receive estrogen therapy displayed a significant decrease in metabolism in the posterior cingulated cortex compared to estrogen users (Rasgon, et al., 2005). Moreover, estrogen therapy (ET) users versus nonusers exhibited significant differences in regional cerebral blood flow relative to activation patterns during memory tasks (Maki and Resnick, 2001). In this study, we demonstrated that OVX induced a significant decrease in PDH and COX activity, the key catalytic machinery required for ATP generation in both nonTg and 3xTgAD mice, which was prevented by E2 treatment initiated at time of OVX.

Oxidative stress closely parallels deficits in mitochondrial bioenergetics and development of AD neuropathology. Increased oxidative modification of key metabolic enzymes will lead to compromised enzyme activity, decreased energy production (Cadenas and Davies, 2000) and increased Aβ production (Hirai, et al., 2001, Moreira, et al., 2007). Estrogen is a key regulator of the antioxidative defense system and can protect against oxidative damage by up-regulation of antioxidant mechanisms, through genomic and non-genomic estrogen signaling pathways (Asthana, et al., 2009, Irwin, et al., 2008, Nilsen, et al., 2007, Vina, et al., 2005). In this study, we demonstrated that OVX significantly increased lipid peroxidation and RNA oxidation, two common oxidative stress markers in AD human patients (Nunomura, et al., 2009, Yang, et al., 2008), whereas E2 treatment initiated at time of OVX prevented the OVX-induced increase in oxidative damage.

Beta amyloid, a pathological marker of AD, accumulates within mitochondria, interacts with a mitochondrial protein, ABAD (Aβ-binding-alcohol-dehydrogenase, HSD17B10, 17β −hydroxysteroid dehydrogenase), and is associated with mitochondrial dysfunction in AD (Lustbader, et al., 2004, Takuma, et al., 2005). We have previously demonstrated that significant accumulation of mitochondrial Aβ first became significant in 9 months old intact female 3xTgAD mice (Yao, et al., 2009). In the current study, OVX significantly increased mitochondrial Aβ load to a level comparable to 9-month-old 3xTgAD animals (Yao, et al., 2009) whereas E2 treatment prevented the OVX-induced increase. In parallel, mitochondrial ABAD expression was increased by OVX and prevented by E2 treatment at time of OVX. Multiple lines of evidence indicate that loss of ovarian hormones can lead to increased generation or decreased clearance of Aβ in brain (Carroll and Pike, 2008, Carroll, et al., 2007, Gandy, et al., 1994, Petanceska, et al., 2000, Zhao, et al., 2010). Increased Aβ in brain following loss of ovarian hormones, first reported by Petanceska and co-workers, is replicated here and in multiple studies (Carroll and Pike, 2008, Carroll, et al., 2007, Zhao, et al., 2010). From a bioenergetic perspective, several reports indicate that decreased mitochondrial bioenergetics coupled with increased oxidative stress contributes to overproduction of Aβ in brain (Grieb, et al., 2004, Velliquette, et al., 2005). This postulate is further supported by findings of Mosconi (Mosconi, et al., 2010) in which individuals with maternal family history of age-related AD exhibited increased brain Aβ burden. Further, Mosconi's earlier work demonstrated that children of mother's with Alzheimer's disease had reduced brain metabolism in AD-vulnerable brain regions, indicating an increased risk of developing the disease relative to individuals with a paternal or no parental history of Alzheimer's disease (Mosconi, et al., 2009). These findings are particularly relevant given that the mitochondrial genome is maternally inherited (Wallace, 2005) and are consistent with earlier reports of a maternal inheritance pattern of AD (Edland, et al., 1996). In addition to Aβ overproduction, loss of ovarian hormones resulted in decreased expression of Aβ degrading enzymes in brain, such as insulin degrading enzyme (IDE) (Zhao, et al., 2010). A decline in IDE would result in decreased Aβ clearance and a concomitant rise in Aβ accumulation, which is prevented by E2 (Carroll and Pike, 2008, Carroll, et al., 2007, Petanceska, et al., 2000, Zhao, et al., 2010).

NIH-PA Author Manuscript

NIH-PA Author Manuscript

NIH-PA Author Manuscript

Changes in mitochondrial bioenergetic capacity could be due to differences in mitochondrial number, size, and density per cell as well as to changes in mitochondrial components, enzyme activity, and consequently altered mitochondrial efficiency. In this study, we demonstrated that OVX induced a significant increase in the fission protein, Drp1, and a significant decrease in the fusion protein, OPA1, suggesting increased mitochondrial fragmentation due to ovarian hormone depletion, whereas E2 treatment prevented the OVX-induced alteration in mitochondrial dynamics. Changes in mitochondrial fission and fusion regulate mitochondrial ultrastructure, such as cristae remodeling, and hence regulate mitochondrial efficiency (Chan, 2006). Unlike the alteration in mitochondrial dynamics, there was no change in mitochondrial DNA content in response to loss of ovarian hormones for the period of this study, suggesting that mitochondrial biogenesis is not impacted by loss of ovarian hormones. Collectively the rise in Aβ localized to mitochondria, the decline in key regulators of the bioenergetic pathway in brain coupled with an increase in oxidative stress and excessive mitochondrial fission could lead to a pathogenic process of synaptic loss, neuronal damage and Alzheimer's pathology (Cho, et al., 2009, Wang, et al., 2009).

In vitro metabolic analysis indicated that E2 differentially regulated mitochondrial bioenergetics in neurons and mixed glia. In neurons, E2 induced an increase in maximal mitochondrial respiratory capacity while not affecting basal respiration, indicating that E2 increased the respiratory capacity of mitochondria necessary for bioenergetically demanding functions such as increased synaptic transmission. In mixed glia, E2 increased both basal and maximal respiratory capacity. As glial cells generate bioenergetic substrates for both neurons and their own energetic demands, the increase in basal respiration is likely due to E2-induced up-regulation of glycolytic pathways in glia which is consistent with previous reports that E2 increases the activity of glycolytic enzymes in rodent brains (Brinton, 2008). The increase in glycolytic activity of glia expands the substrate reservoir for high-energy demanding conditions. Together, these findings indicate that E2 promotes the maximal reserved mitochondrial respiratory capacity of neurons while simultaneously increasing the capacity of glia to respond to increased demands of metabolic substrates coupled with increased neuronal activity. Coordination of enhanced neuronal metabolic activity with enlarged glial capacity to provide substrates to fuel demands is critical to sustain highly active neural networks and maintain glutamaterigic homeostasis that occurs during E2 enhancement of long-term potentiation (Brinton, 2008, Brinton, 2009)

Clinically, the impact of hormone interventions and the association with risk of AD has been fraught with controversy. This state of controversy is diminishing as a clearer understanding of the neurobiological mechanisms underlying the disparities in response to hormone therapies. Findings from previous studies indicate a healthy cell bias of estrogen action, which predicts that under conditions of optimal cell viability estrogen promotes mechanisms of neuron survival, neuron metabolism and neuronal function (Brinton, 2008, Henderson, 2010). In contrast, when cells have compromised viability, exposure to estrogen can exacerbate the demise of cells in response to neurodegenerative insults. These basic science findings are consistent with clinical data indicating a window of opportunity for efficacy of hormone therapy, which is articulated in the timing hypothesis (Henderson, 2010, Rocca, et al., 2010). Consistent with previous epidemiological findings (Yaffe, et al., 2007), recent clinical analyses indicate that hormone therapy intervention at the time of the menopausal transition, when neurological viability is still intact, reduced the risk of developing Alzheimer's disease in women (Berent-Spillson, et al., 2010, Maki, et al., 2010, Whitmer, et al., 2010). In contrast, intervention in women many years post menopause resulted in an increased risk of AD (Shumaker, et al., 2003), which is consistent with the results of the Cache County Study (Zandi, et al., 2002). Collectively, basic science and clinical findings are converging to indicate that loss of ovarian hormones can increase the risk of hypometabolism in brain thereby creating a state of neurological vulnerability which has

NIH-PA Author Manuscript

NIH-PA Author Manuscript

NIH-PA Author Manuscript

implications for risk of developing late-onset Alzheimer's disease. Further, introduction of ovarian hormones to sustain neurological function in a healthy brain prior to development of neurological impairment is consistent of the healthy bias of estrogen action and the window of opportunity for therapeutic efficacy.

In summary, loss of ovarian hormones due to ovariectomy induced a significant decline in mitochondrial bioenergetic function in nonTg mice and exacerbated the impairment of mitochondrial bioenergetics in 3xTgAD mice. In young ovariectomized nonTg mice, the impairment of mitochondrial bioenergetics approached a level comparable to older reproductively senescent mice (Yao, et al., 2009) and young 3xTgAD mice. Thus, the loss of ovarian hormones either through naturally occurring reproductive senescence or surgical OVX induces an accelerated aging phenotype. Findings from this study support our hypothesis that loss of ovarian hormones accelerates the decline in mitochondrial bioenergetics, linking the loss of ovarian hormones to the development of a hypometabolic brain phenotype clinically observed in menopausal women (Maki and Resnick, 2000, Rasgon, et al., 2005) and prodromal AD brains (Reiman, 2007). Together with our previous findings that mitochondrial bioenergetic deficits precede the appearance of AD pathology (Yao, et al., 2009), results of the current study suggest a plausible mechanism underlying the increased lifetime risk for developing AD in menopausal and premenopausally oophorectomized women.

Acknowledgments

This study was supported by National Institute on Aging Grant 2R01AG032236 (to RDB) National Institute on Aging Grant 5P01AG026572 (Project 1 to EC and RDB) and Eileen L. Norris Foundation (to RDB). We gratefully acknowledge gift of triple-transgenic Alzheimer's disease mouse model from Dr. Frank M Laferla.

References

Alzheimer's, Association. 2010 Alzheimer's Disease Facts and Figures Alzheimer's & Dementia 6. 2010

Asthana S, Brinton RD, Henderson VW, McEwen BS, Morrison JH, Schmidt PJ. Frontiers proposal. National Institute on Aging "bench to bedside: estrogen as a case study". Age (Dordr). 2009; 31(3): 199–210. [PubMed: 19277902]

Beal MF. Mitochondria take center stage in aging and neurodegeneration. Ann Neurol. 2005; 58(4): 495–505. [PubMed: 16178023]

Belanger M, Magistretti PJ. The role of astroglia in neuroprotection. Dialogues Clin Neurosci. 2009; 11(3):281–295. [PubMed: 19877496]

Berent-Spillson A, Persad CC, Love T, Tkaczyk A, Wang H, Reame NK, Frey KA, Zubieta JK, Smith YR. Early menopausal hormone use influences brain regions used for visual working memory. Menopause. 2010; 17(4):692–699. [PubMed: 20300040]

Blass JP, Sheu RK, Gibson GE. Inherent abnormalities in energy metabolism in Alzheimer disease. Interaction with cerebrovascular compromise. Ann. NY. Acad. Sci. 2000; 903:204–221. [PubMed: 10818509]

Brinton RD. The healthy cell bias of estrogen action: mitochondrial bioenergetics and neurological implications. Trends Neurosci. 2008; 31(10):529–537. [PubMed: 18774188]

Brinton RD. Estrogen-induced plasticity from cells to circuits: predictions for cognitive function. Trends Pharmacol Sci. 2009; 30(4):212–22. 10.1016/j.tips.2008.12.006. [PubMed: 19299024]

Cadenas E, Davies KJ. Mitochondrial free radical generation, oxidative stress, and aging. Free Radic Biol Med. 2000; 29(3–4):222–230. [PubMed: 11035250]

Carroll JC, Pike CJ. Selective estrogen receptor modulators differentially regulate Alzheimer-like changes in female 3xTg-AD mice. Endocrinology. 2008; 149(5):2607–2611. 10.1210/en.2007-1346. [PubMed: 18276750]

NIH-PA Author Manuscript

NIH-PA Author Manuscript

NIH-PA Author Manuscript

Carroll JC, Rosario ER, Chang L, Stanczyk FZ, Oddo S, LaFerla FM, Pike CJ. Progesterone and estrogen regulate Alzheimer-like neuropathology in female 3xTg-AD mice. J Neurosci. 2007; 27(48):13357–13365. 10.1523/JNEUROSCI.2718-07.2007. [PubMed: 18045930]

Chan DC. Mitochondria: dynamic organelles in disease, aging, and development. Cell. 2006; 125(7): 1241–1252. [PubMed: 16814712]

Cho DH, Nakamura T, Fang J, Cieplak P, Godzik A, Gu Z, Lipton SA. S-nitrosylation of Drp1 mediates beta-amyloid-related mitochondrial fission and neuronal injury. Science. 2009; 324(5923):102–105. 10.1126/science.1171091. [PubMed: 19342591]

Edland SD, Silverman JM, Peskind ER, Tsuang D, Wijsman E, Morris JC. Increased risk of dementia in mothers of Alzheimer's disease cases: evidence for maternal inheritance. Neurology. 1996; 47(1):254–256. [PubMed: 8710088]

Gandy S, Caporaso G, Buxbaum J, Frangione B, Greengard P. APP processing, A beta-amyloidogenesis, and the pathogenesis of Alzheimer's disease. Neurobiol Aging. 1994; 15(2):253–256. [PubMed: 7838304]

Grieb P, Gordon-Krajcer W, Frontczak-Baniewicz M, Walski M, Ryba MS, Kryczka T, Fiedorowicz M, Kulinowski P, Sulek Z, Majcher K, Jasinski A. 2-deoxyglucose induces beta-APP overexpression, tau hyperphosphorylation and expansion of the trans-part of the Golgi complex in rat cerebral cortex. Acta neurobiologiae experimentalis. 2004; 64(4):491–502. [PubMed: 15586666]

Henderson VW, RD. Menopause and Mitochondria: Windows into Estrogen Effects on Alzheimer's Disease Risk and Therapy: Progress in Brain Research. Neuroendocrinology. 2010; 182:77–96.

Hirai K, Aliev G, Nunomura A, Fujioka H, Russell RL, Atwood CS, Johnson AB, Kress Y, Vinters HV, Tabaton M, Shimohama S, Cash AD, Siedlak SL, Harris PL, Jones PK, Petersen RB, Perry G, Smith MA. Mitochondrial abnormalities in Alzheimer's disease. J Neurosci. 2001; 21(9):3017–3023. [PubMed: 11312286]

Irwin RW, Yao J, Hamilton RT, Cadenas E, Brinton RD, Nilsen J. Progesterone and estrogen regulate oxidative metabolism in brain mitochondria. Endocrinology. 2008; 149(6):3167–3175. [PubMed: 18292191]

Lopez-Grueso R, Borras C, Gambini J, Vina J. Aging and ovariectomy cause a decrease in brain glucose consumption in vivo in Wistar rats. Rev Esp Geriatr Gerontol. 2010; 45(3):136–140. 10.1016/j.regg.2009.12.005. [PubMed: 20206415]

Lustbader JW, Cirilli M, Lin C, Xu HW, Takuma K, Wang N, Caspersen C, Chen X, Pollak S, Chaney M, Trinchese F, Liu S, Gunn-Moore F, Lue LF, Walker DG, Kuppusamy P, Zewier ZL, Arancio O, Stern D, Yan SS, Wu H. ABAD directly links Abeta to mitochondrial toxicity in Alzheimer's disease. Science. 2004; 304(5669):448–452. [PubMed: 15087549]

Magistretti PJ. Neuron-glia metabolic coupling and plasticity. J Exp Biol. 2006; 209(Pt 12):2304–2311. 10.1242/jeb.02208. [PubMed: 16731806]

Maki PM, Dennerstein L, Clark M, Guthrie J, Lamontagne P, Fornelli D, Little D, Henderson VW, Resnick SM. Perimenopausal use of hormone therapy is associated with enhanced memory and hippocampal function later in life. Brain Res. 2010 10.1016/j.brainres.2010.11.030.

Maki PM, Resnick SM. Longitudinal effects of estrogen replacement therapy on PET cerebral blood flow and cognition. Neurobiol Aging. 2000; 21(2):373–383. [PubMed: 10867223]

Maki PM, Resnick SM. Effects of estrogen on patterns of brain activity at rest and during cognitive activity: a review of neuroimaging studies. Neuroimage. 2001; 14(4):789–801. S1053-8119(01)90887-0 [pii]. [PubMed: 11554798]

Martins RN, Hallmayer J. Age at onset: important marker of genetic heterogeneity in Alzheimer's disease. The pharmacogenomics journal. 2004; 4(3):138–140. [PubMed: 15024381]

Moreira PI, Santos MS, Seica R, Oliveira CR. Brain mitochondrial dysfunction as a link between Alzheimer's disease and diabetes. J Neurol Sci. 2007; 257(1–2):206–214. [PubMed: 17316694]

Moreira PI, Zhu X, Wang X, Lee HG, Nunomura A, Petersen RB, Perry G, Smith MA. Mitochondria: a therapeutic target in neurodegeneration. Biochim Biophys Acta. 2010; 1802(1):212–220. 10.1016/j.bbadis.2009.10.007. [PubMed: 19853657]

Mosconi L, Mistur R, Switalski R, Brys M, Glodzik L, Rich K, Pirraglia E, Tsui W, De Santi S, de Leon MJ. Declining brain glucose metabolism in normal individuals with a maternal history of

NIH-PA Author Manuscript

NIH-PA Author Manuscript

NIH-PA Author Manuscript

Alzheimer disease. Neurology. 2009; 72(6):513–520. 10.1212/01.wnl.0000333247.51383.43. [PubMed: 19005175]

Mosconi L, Rinne JO, Tsui WH, Berti V, Li Y, Wang H, Murray J, Scheinin N, Nagren K, Williams S, Glodzik L, De Santi S, Vallabhajosula S, de Leon MJ. Increased fibrillar amyloid-{beta} burden in normal individuals with a family history of late-onset Alzheimer's. Proc. Natl. Acad. Sci. U. S. A. 2010; 107(13):5949–5954. 10.1073/pnas.0914141107. [PubMed: 20231448]

Mosconi L, Sorbi S, de Leon MJ, Li Y, Nacmias B, Myoung PS, Tsui W, Ginestroni A, Bessi V, Fayyazz M, Caffarra P, Pupi A. Hypometabolism exceeds atrophy in presymptomatic early-onset familial Alzheimer's disease. J Nucl Med. 2006; 47(11):1778–1786. [PubMed: 17079810]

Nicholson RM, Kusne Y, Nowak LA, Laferla FM, Reiman EM, Valla J. Regional cerebral glucose uptake in the 3xTG model of Alzheimer's disease highlights common regional vulnerability across AD mouse models. Brain Res. 2010 10.1016/j.brainres.2010.05.084.

Nilsen J, Irwin RW, Gallaher TK, Brinton RD. Estradiol in vivo regulation of brain mitochondrial proteome. J Neurosci. 2007; 27(51):14069–14077. [PubMed: 18094246]

Nunomura A, Hofer T, Moreira PI, Castellani RJ, Smith MA, Perry G. RNA oxidation in Alzheimer disease and related neurodegenerative disorders. Acta neuropathologica. 2009; 118(1):151–166. [PubMed: 19271225]

Oddo S, Caccamo A, Shepherd JD, Murphy MP, Golde TE, Kayed R, Metherate R, Mattson MP, Akbari Y, LaFerla FM. Triple-transgenic model of Alzheimer's disease with plaques and tangles: intracellular Abeta and synaptic dysfunction. Neuron. 2003; 39(3):409–421. [PubMed: 12895417]

Petanceska SS, Nagy V, Frail D, Gandy S. Ovariectomy and 17beta-estradiol modulate the levels of Alzheimer's amyloid beta peptides in brain. Neurology. 2000; 54(12):2212–2217. [PubMed: 10881241]

Rasgon NL, Silverman D, Siddarth P, Miller K, Ercoli LM, Elman S, Lavretsky H, Huang SC, Phelps ME, Small GW. Estrogen use and brain metabolic change in postmenopausal women. Neurobiol Aging. 2005; 26(2):229–235. [PubMed: 15582750]

Reddy PH, Beal MF. Amyloid beta, mitochondrial dysfunction and synaptic damage: implications for cognitive decline in aging and Alzheimer's disease. Trends Mol. Med. 2008; 14(2):45–53. [PubMed: 18218341]

Reiman EM. Linking brain imaging and genomics in the study of Alzheimer's disease and aging. Ann. NY. Acad. Sci. 2007; 1097:94–113. 10.1196/annals.1379.011. [PubMed: 17413015]

Reiman EM, Chen K, Alexander GE, Caselli RJ, Bandy D, Osborne D, Saunders AM, Hardy J. Correlations between apolipoprotein E epsilon4 gene dose and brain-imaging measurements of regional hypometabolism. Proc. Natl. Acad. Sci. U. S. A. 2005; 102(23):8299–8302. 10.1073/pnas.0500579102. [PubMed: 15932949]

Rocca WA, Bower JH, Maraganore DM, Ahlskog JE, Grossardt BR, de Andrade M, Melton Iii LJ. Increased risk of cognitive impairment or dementia in women who underwent oophorectomy before menopause. Neurology. 2007

Rocca WA, Grossardt BR, Shuster LT. Oophorectomy, Menopause, Estrogen, and Cognitive Aging: The Timing Hypothesis. Neurodegener Dis. 2010; 7(1–3):163–166. 10.1159/000289229. [PubMed: 20197698]

Shumaker SA, Legault C, Rapp SR, Thal L, Wallace RB, Ockene JK, Hendrix SL, Jones BN 3rd, Assaf AR, Jackson RD, Kotchen JM, Wassertheil-Smoller S, Wactawski-Wende J. Estrogen plus progestin and the incidence of dementia and mild cognitive impairment in postmenopausal women: the Women's Health Initiative Memory Study: a randomized controlled trial. JAMA. 2003; 289(20):2651–2662. 289/20/2651 [pii]. [PubMed: 12771112]

Simpkins JW, Dykens JA. Mitochondrial mechanisms of estrogen neuroprotection. Brain Res Rev. 2008; 57(2):421–430. 10.1016/j.brainresrev.2007.04.007. [PubMed: 17512984]

Simpkins JW, Yi KD, Yang SH, Dykens JA. Mitochondrial mechanisms of estrogen neuroprotection. Biochim Biophys Acta. 2009 10.1016/j.bbagen.2009.11.013.

Swerdlow RH, Khan SM. The Alzheimer's disease mitochondrial cascade hypothesis: an update. Exp Neurol. 2009; 218(2):308–315. 10.1016/j.expneurol.2009.01.011. [PubMed: 19416677]

NIH-PA Author Manuscript

NIH-PA Author Manuscript

NIH-PA Author Manuscript

Takuma K, Yao J, Huang J, Xu H, Chen X, Luddy J, Trillat AC, Stern DM, Arancio O, Yan SS. ABAD enhances Abeta-induced cell stress via mitochondrial dysfunction. FASEB J. 2005; 19(6): 597–598. [PubMed: 15665036]

Velliquette RA, O'Connor T, Vassar R. Energy inhibition elevates beta-secretase levels and activity and is potentially amyloidogenic in APP transgenic mice: possible early events in Alzheimer's disease pathogenesis. J Neurosci. 2005; 25(47):10874–10883. [PubMed: 16306400]

Vina J, Borras C, Gambini J, Sastre J, Pallardo FV. Why females live longer than males? Importance of the upregulation of longevity-associated genes by oestrogenic compounds. FEBS Lett. 2005; 579(12):2541–2545. [PubMed: 15862287]

Wallace DC. A mitochondrial paradigm of metabolic and degenerative diseases, aging, and cancer: a dawn for evolutionary medicine. Annu Rev Genet. 2005; 39:359–407. [PubMed: 16285865]

Wang X, Su B, Lee HG, Li X, Perry G, Smith MA, Zhu X. Impaired balance of mitochondrial fission and fusion in Alzheimer's disease. J Neurosci. 2009; 29(28):9090–9103. 10.1523/JNEUROSCI.1357-09.2009. [PubMed: 19605646]

Whitmer RA, Quesenberry CP, Zhou J, Yaffe K. Timing of hormone therapy and dementia: The critical window theory revisited. Ann Neurol. 2010

Will Y, Hynes J, Ogurtsov VI, Papkovsky DB. Analysis of mitochondrial function using phosphorescent oxygen-sensitive probes. Nature protocols. 2006; 1(6):2563–2572.

Yaffe K, Barnes D, Lindquist K, Cauley J, Simonsick EM, Penninx B, Satterfield S, Harris T, Cummings SR. Endogenous sex hormone levels and risk of cognitive decline in an older biracial cohort. Neurobiol Aging. 2007; 28(2):171–178. 10.1016/j.neurobiolaging.2006.10.004. [PubMed: 17097195]

Yang JL, Weissman L, Bohr VA, Mattson MP. Mitochondrial DNA damage and repair in neurodegenerative disorders. DNA Repair (Amst). 2008; 7(7):1110–1120. 10.1016/j.dnarep.2008.03.012. [PubMed: 18463003]

Yao J, Hamilton RT, Cadenas E, Brinton RD. Decline in mitochondrial bioenergetics and shift to ketogenic profile in brain during reproductive senescence. Biochim Biophys Acta. 2010 10.1016/j.bbagen.2010.06.002.

Yao J, Irwin RW, Zhao L, Nilsen J, Hamilton RT, Brinton RD. Mitochondrial bioenergetic deficit precedes Alzheimer's pathology in female mouse model of Alzheimer's disease. Proc. Natl. Acad. Sci. U. S. A. 2009; 106(34):14670–14675. [PubMed: 19667196]

Zandi PP, Carlson MC, Plassman BL, Welsh-Bohmer KA, Mayer LS, Steffens DC, Breitner JC. Hormone replacement therapy and incidence of Alzheimer disease in older women: the Cache County Study. JAMA. 2002; 288(17):2123–2129. [PubMed: 12413371]

Zhao L, Yao J, Mao Z, Chen S, Wang Y, Brinton RD. 17beta-Estradiol regulates insulin-degrading enzyme expression via an ERbeta/PI3-K pathway in hippocampus: Relevance to Alzheimer's prevention. Neurobiol Aging. 2010 10.1016/j.neurobiolaging.2009.12.010.

NIH-PA Author Manuscript
NIH-PA Author Manuscript
NIH-PA Author Manuscript

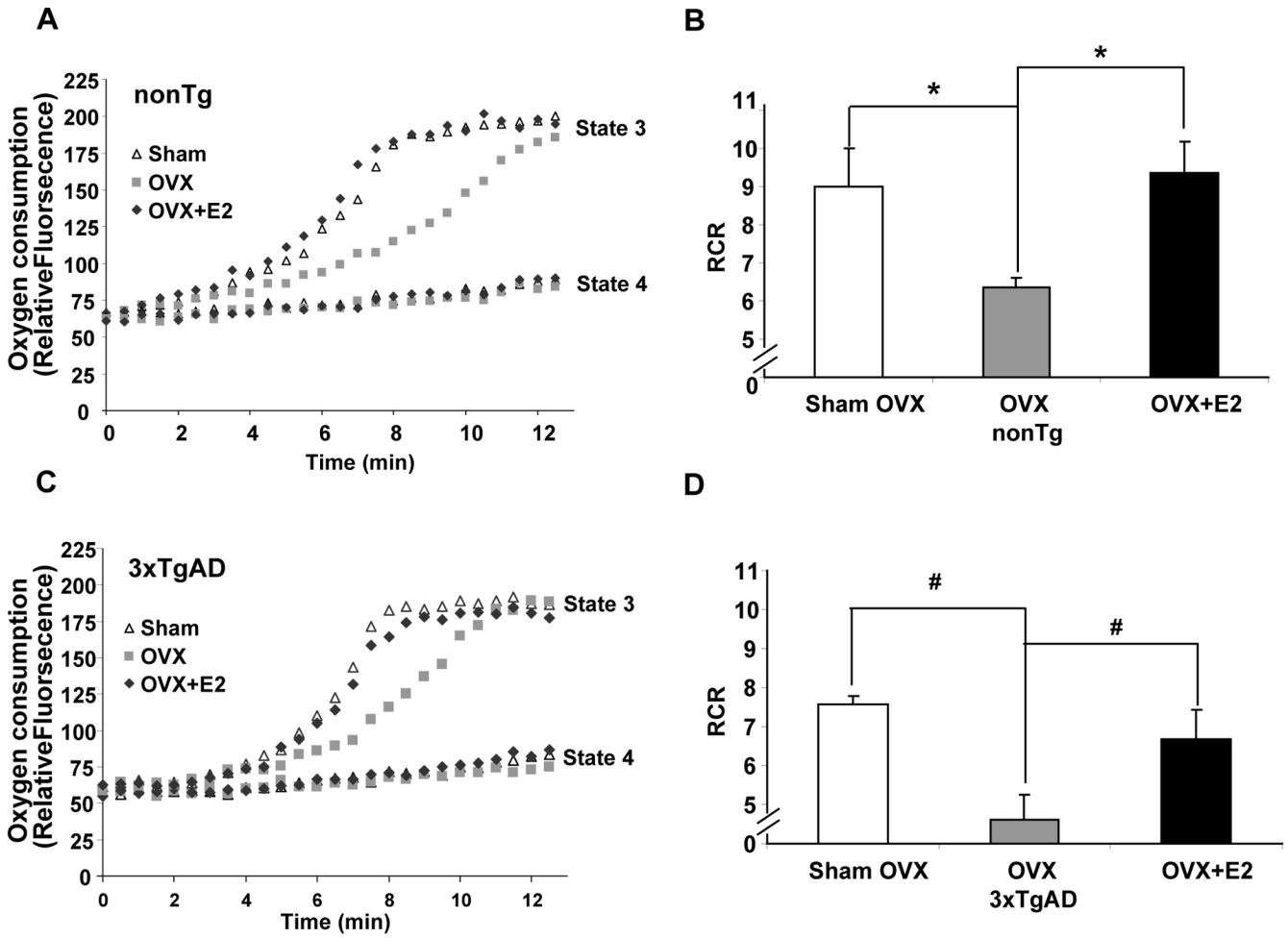

Figure 1. OVX induced decrease in mitochondrial respiration and prevention by 17β-estradiol

Whole brain mitochondria were isolated from Sham-OVX, OVX, and OVX+E2 group for both nonTg and 3xTgAD mice at the end of the treatment. State 3/State 4 respiration was determined using the Luxcel MitoXpress Oxygen-sensitive Fluorescent assay. State 4 mitochondrial respiration was measured in the presence of L-malate (5 mM), L-glutamate (5 mM); State 3 mitochondrial respiration was measured in the presence of L-malate (5 mM), L-glutamate (5 mM), plus ADP (410 μM). The Respiratory Control Ratio (RCR) is defined as State 3/State 4 respiration. A&C, representative curves for State 3 and State 4 brain mitochondrial respiration for nonTg and 3xTgAD mice, respectively. B&D, OVX significantly decreased RCR in both nonTg (B) and 3xTgAD (D) mice, whereas E2 treatment initiated at time of OVX prevented the OVX induced decrease. (Bars represent mean value ± S.E.M *, P<0.05 compared to the nonTg OVX group, #, P<0.05 compared to the 3xTgAD OVX group, n=7)

NIH-PA Author Manuscript
NIH-PA Author Manuscript
NIH-PA Author Manuscript

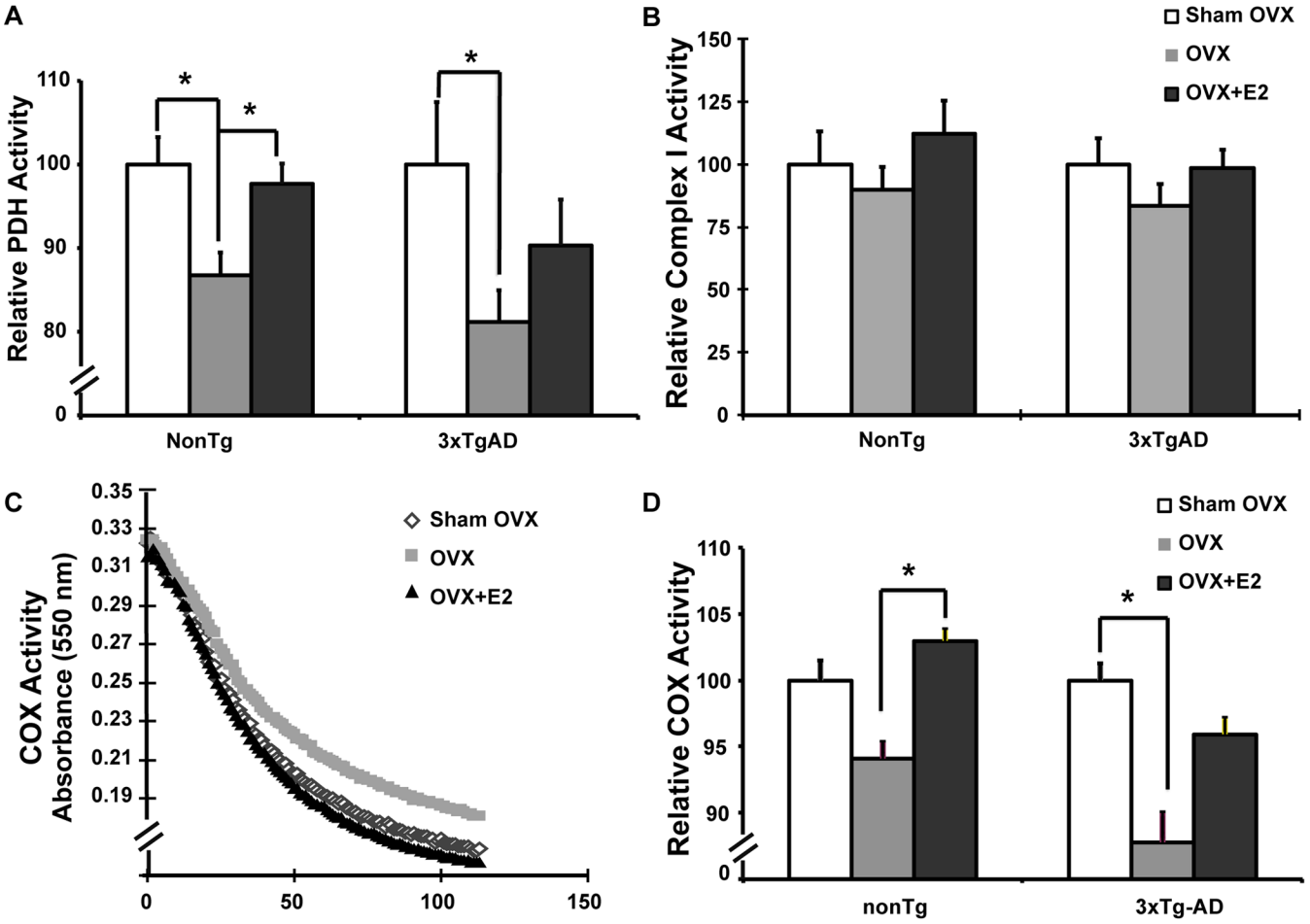

Figure 2. OVX induced decrease in mitochondrial enzyme activity and prevention by 17β-estradiol

Brain mitochondria isolated from Sham-OVX, OVX, OVX+E2 groups of both nonTg and 3xTg-AD mice were assessed for PDH, Complex I and Complex IV (COX) activities respectively. A, OVX induced decrease in PDH activity and prevention by 17β-estradiol, relative PDH activity was calculated as the relative value normalized to the Sham-OVX group of the same genotype; B, no significant change in complex I activity with OVX or OVX+E2 treatment, relative Complex I activity was calculated as the relative value normalized to the Sham-OVX group of the same genotype; C, representative COX activity curve of 3xTgAD mice; D, OVX induced decrease in COX activity and prevention by 17β-estradiol, relative COX activity was calculated as the relative value normalized to the Sham-OVX group of the same genotype. Bars represent mean enzyme activity value ± SEM (*, $P<0.05$ compared to nonTg OVX group, #, $P<0.05$compared to 3xTgAD OVX group, n=7)

NIH-PA Author Manuscript

NIH-PA Author Manuscript

NIH-PA Author Manuscript

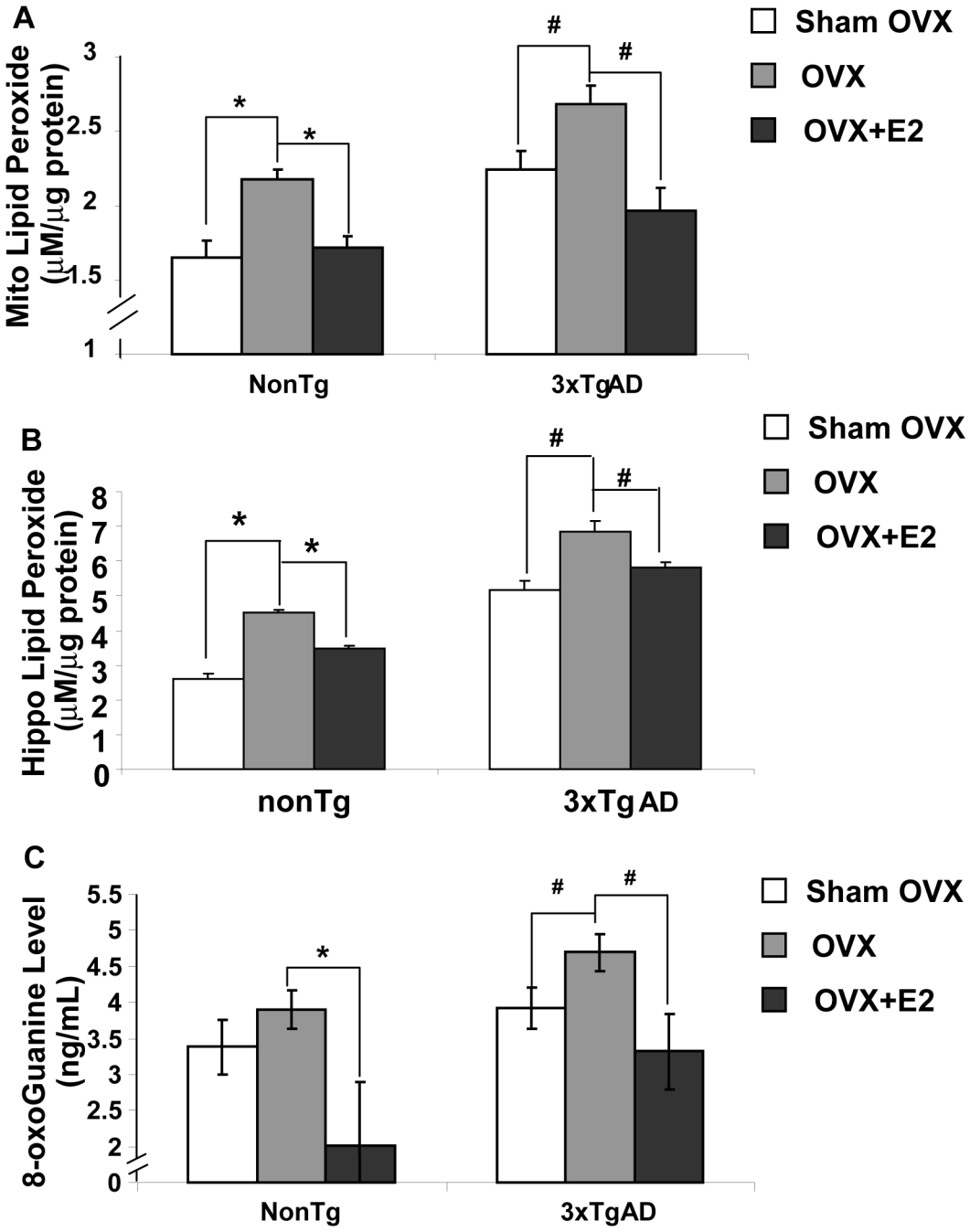

Figure 3. OVX induced increase in oxidative stress and prevention by 17β-estradiol

Brain mitochondria were isolated and serum samples were collected from Sham-OVX, OVX, OVX+E2 groups of both nonTg and 3xTg-AD mice. Lipid peroxide levels were determined by the leucomethylene blue assay. Serum 8-oxoGuanine levels were determined with the 8-oxoGuanine assay kit. A, OVX induced increased in mitochondrial lipid peroxidation and prevention by 17β-estradiol; B, OVX induced increased in hippocampal lipid peroxidation and prevention by 17β-estradiol; C, OVX induced significant increase in serum 8-oxoGuanine level and prevention by 17β-estradiol. Bars represent mean value ± S.E.M. (*, P<0.05 compared to nonTg OVX group; #, P<0.05 compared to3xTgAD OVX group, n=7)

NIH-PA Author Manuscript

NIH-PA Author Manuscript

NIH-PA Author Manuscript

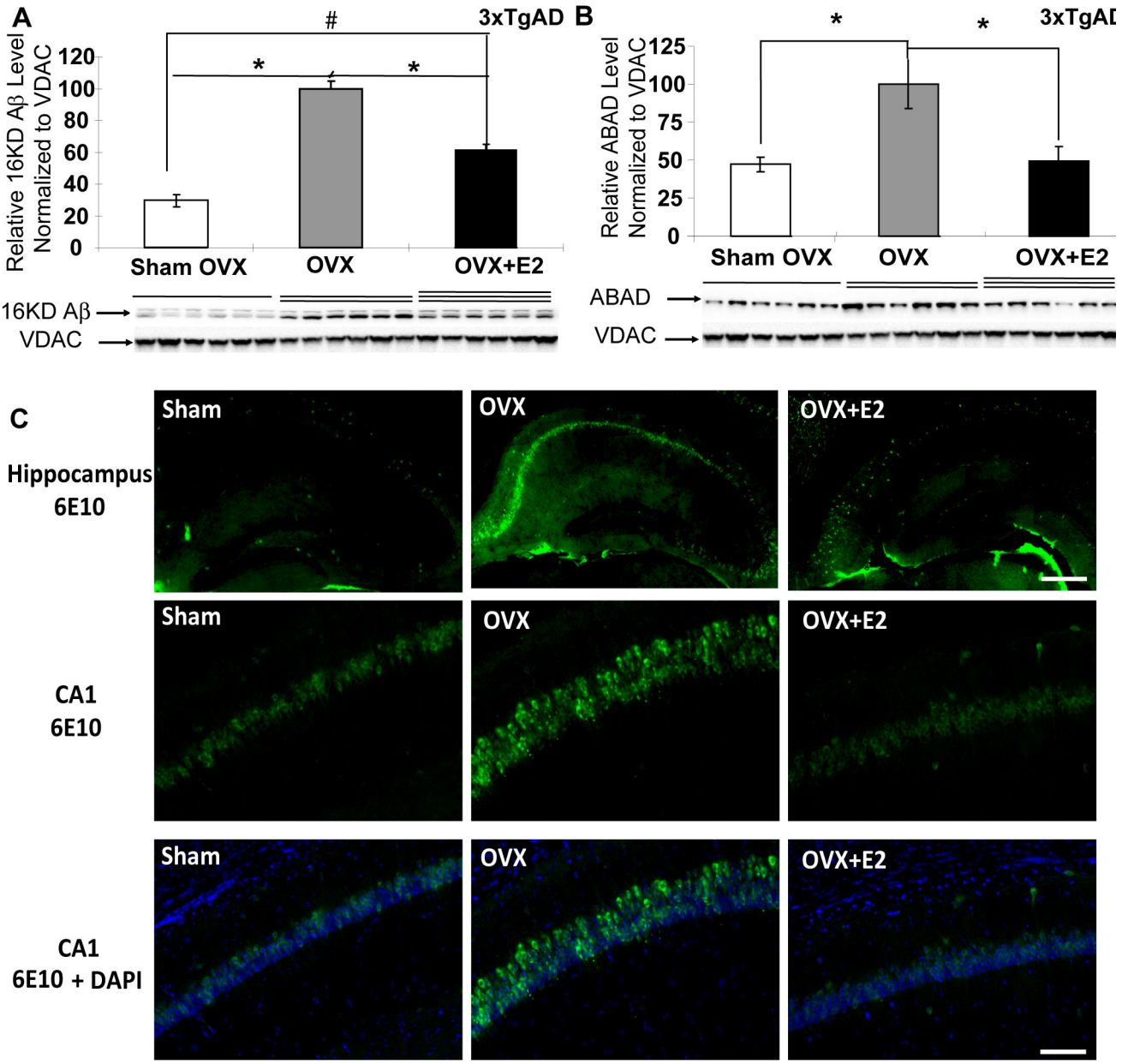

Figure 4. OVX induced increase in mitochondrial and hippocampal amyloid load and prevention by 17β-estradiol

Equal amount of mitochondrial samples isolated from Sham-OVX, OVX, and OVX+E2 groups of 3xTg-AD mice were loaded onto the gel. Expression of mitochondrial 16 kD Aβ oligomer and ABAD protein was determined by Western blot analysis. A, OVX induced significant increase in mitochondrial 16 kD Aβ level and partial prevention by E2; B, OVX induced significant increase in mitochondrial ABAD expression and prevention by E2 (Bars represent mean relative expression ± S.E.M., *, $P<0.05$ compared to the 3xTgAD OVX group, n=6; #, $P<0.05$ compared to the 3xTgAD Sham-OVX group). C, OVX induced significant increase in hippocampal Aβ IR and prevention by E2. Brain hemispheres were sectioned at 30μm. Aβ IR was detected with 6E10 antibody (green) with nuclei counter staining with DAPI (blue), Top row, representative images showing Aβ-IR in the

hippocampus, scale: 200 μm; middle row representative images showing Aβ-IR in the CA1 region; bottom row, co-staining of Aβ-IR and nuclei in the CA1 region, scale: 100 μm.

NIH-PA Author Manuscript
NIH-PA Author Manuscript
NIH-PA Author Manuscript

NIH-PA Author Manuscript
NIH-PA Author Manuscript
NIH-PA Author Manuscript

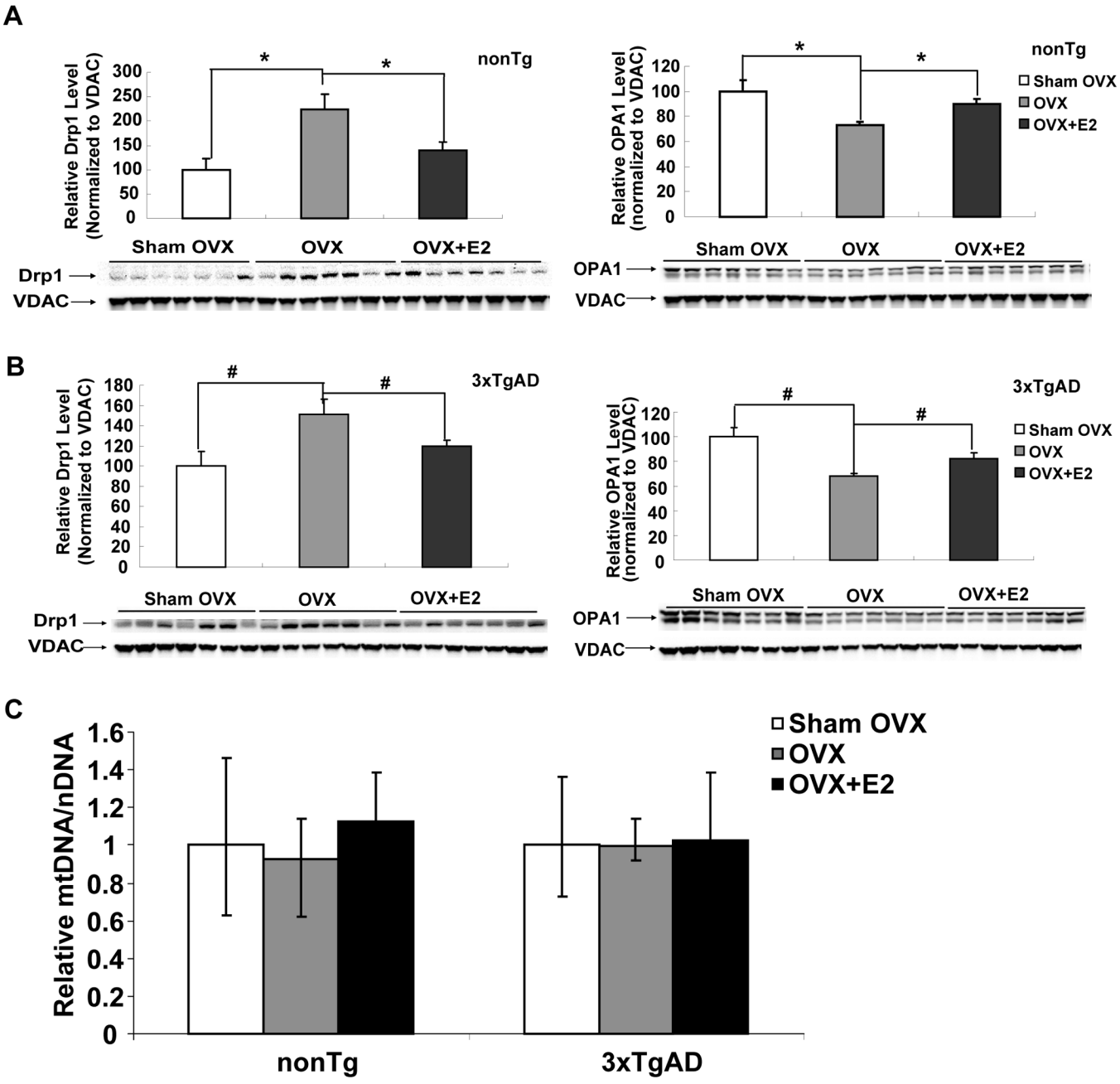

Figure 5. OVX induced alteration of mitochondrial dynamics and prevention by 17β-estradiol

Equal amount of mitochondrial samples isolated from Sham-OVX, OVX, and OVX+E2 groups of both nonTg and 3xTg-AD mice were loaded onto the gel. Expression of mitochondrial Drp1 (fission) and OPA1 (fusion) protein was determined by western blot analysis. A&B, OVX induced significant increase in Drp1 expression and decrease in OPA1 expression in nonTg and 3xTgAD mitochondria, respectively. (*, $P<0.05$ compared to nonTg OVX group; #, $P<0.05$ compared to 3xTgAD OVX group). C, no impact of OVX or E2 treatment on mitochondrial biogenesis. Total DNA was isolated from cortical tissues of Sham-OVX, OVX, and OVX+E2 groups of both nonTg and 3xTg-AD mice. Samples were analyzed by real-time PCR. Mitochondrial content was estimated as the relative levels of COXII DNA (mtDNA) to β-actin (nDNA).

NIH-PA Author Manuscript
NIH-PA Author Manuscript
NIH-PA Author Manuscript

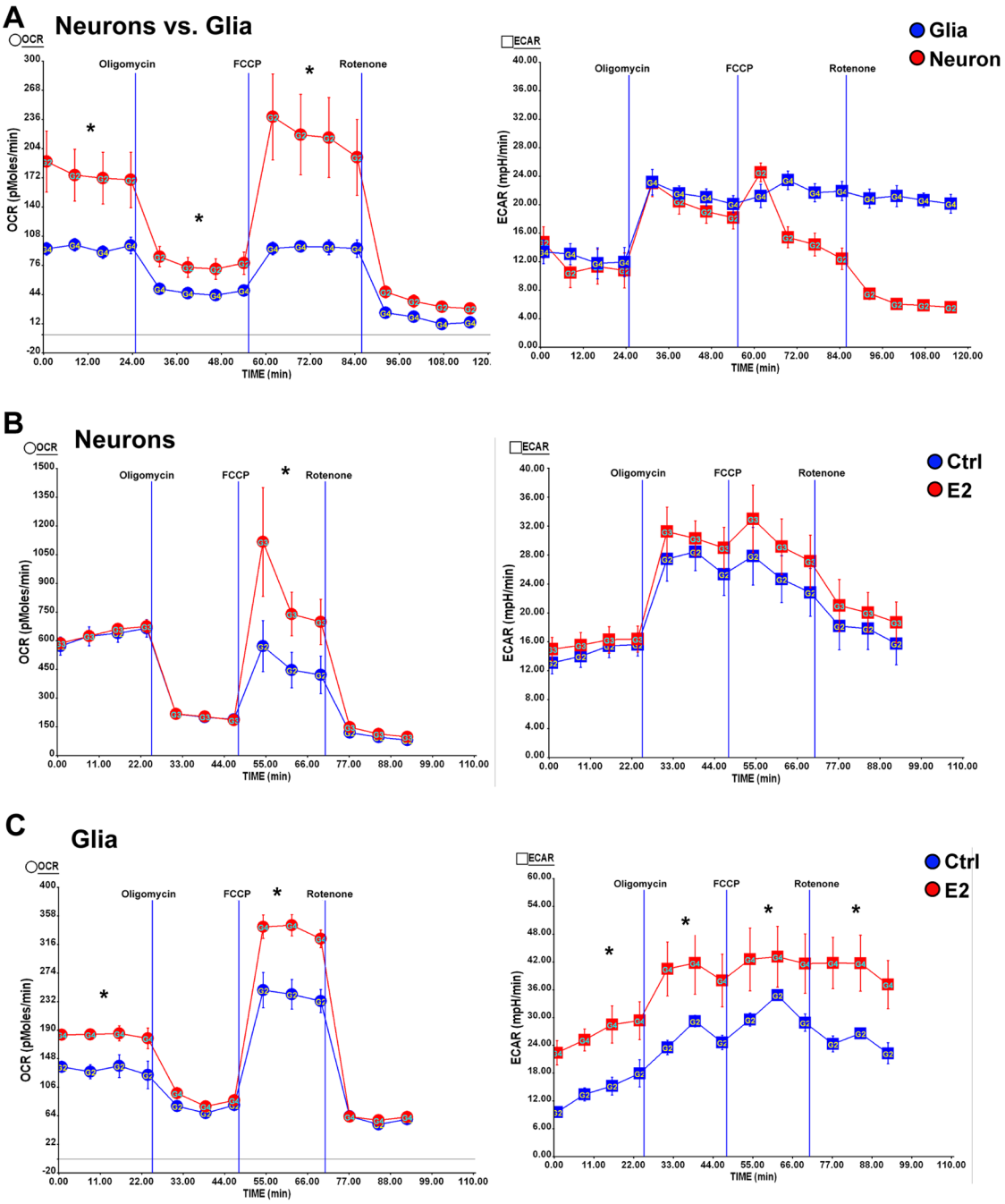

Figure 6. Estrogen differentially regulates mitochondrial bioenergetics in neurons and glia

Primary hippocampal neurons from day 18 (E18) embryos of female Sprague-Dawley rats were cultured in Neurobasal medium + B27 supplement for 10 days prior to experiment. Mixed glia from day 18 (E18) embryos of female Sprague-Dawley rats were cultured in growth media (DMEM:F12 (1:1)+10% FBS). Primary Oxygen consumption rate (OCR) and extracellular acidification rate (ECAR) were determined using the Seahorse XF-24 Metabolic Flux analyzer. Vertical lines indicate time of addition of mitochondrial inhibitors A: oligomycin (1 μM), B: FCCP (1 μM) or C: rotenone (1 μM). A, left panel: higher basal OCR rates and larger maximal mitochondrial respiratory capacity in primary neurons (red) than mixed glia (blue); right panel: comparable glycolysis rate (indicated by ECAR)

between neurons (red) and mixed glia (Blue) (*, P<0.05 compared to mixed glia, n=5 wells per group); B, left panel: E2 treatment (red) increased the maximal mitochondrial respiratory capacity but not the basal respiration in neurons; right panel: E2 treatment did not significantly increase glycolysis (indicated by ECAR) in neurons (*, P<0.05 compared to control (blue), n=5 wells per group); C, left panel: E2 treatment (red) significantly increased both the basal respiration and the maximal mitochondrial respiratory capacity in mixed glia; right panel: E2 treatment (red) significantly increased glycolysis (indicated by ECAR) in mixed glia (*, P<0.05 compared to control (blue), n=5 wells per group).

NIH-PA Author Manuscript
NIH-PA Author Manuscript
NIH-PA Author Manuscript

NIH-PA Author Manuscript

NIH-PA Author Manuscript

NIH-PA Author Manuscript

Table 1

Uterine weight change with estrogen status

Uteri were collected at sacrifice from Sham-OVX, OVX, OVX+E2 groups of both nonTg and 3xTg-AD mice and weighed respectively.

Uterine Weight (g)	Sham OVX	OVX	OVX+E2
nonTg	0.0938± 0.00855 *	0.0255± 0.00534	0.242± 0.0485 *
3xTgAD	0.0936± 0.0101 #	0.0300± 0.00761	0.150± 0.0494 #

Values represent mean uterine weight ± SEM

* P<0.05 compared to nonTg OVX group;

# P<0.05 compared to 3xTgAD OVX group, n=10.